JACS
JOURNAL OF THE AMERICAN CHEMICAL SOCIETY

ARTICLE

pubs.acs.org/JACS

Benzene under High Pressure: a Story of Molecular Crystals Transforming to Saturated Networks, with a Possible Intermediate Metallic Phase

Xiao-Dong Wen,[†] Roald Hoffmann,* and N. W. Ashcroft

Baker Laboratory, Department of Chemistry and Chemical Biology, and Laboratory of Atomic and Solid State Physics and Cornell Center for Materials Research, Clark Hall, Cornell University, Ithaca, New York 14853, United States

Supporting Information

ABSTRACT: In a theoretical study, benzene is compressed up to 300 GPa. The transformations found between molecular phases generally match the experimental findings in the moderate pressure regime (<20 GPa): phase I (*Pbca*) is found to be stable up to 4 GPa, while phase II ($P4_32_12$) is preferred in a narrow pressure range of 4−7 GPa. Phase III ($P2_1/c$) is at lowest enthalpy at higher pressures. Above 50 GPa, phase V ($P2_1$ at 0 GPa; $P2_1/c$ at high pressure) comes into play, slightly more stable than phase III in the range of 50−80 GP, but unstable to rearrangement to a saturated, four-coordinate (at C), one-dimensional polymer. Actually, throughout the entire pressure range, crystals of graphane possess lower enthalpy than molecular benzene structures; a simple thermochemical argument is given for why this is so. In several of the benzene phases there nevertheless are substantial barriers to rearranging the molecules to a saturated polymer, especially at low temperatures. Even at room temperature these barriers should allow one to study the effect of pressure on the metastable molecular phases. Molecular phase III ($P2_1/c$) is one such; it remains metastable to higher pressures up to ~200 GPa, at which point it too rearranges spontaneously to a saturated, tetracoordinate CH polymer. At 300 K the isomerization transition occurs at a lower pressure. Nevertheless, there may be a narrow region of pressure, between P = 180 and 200 GPa, where one could find a metallic, molecular benzene state. We explore several lower dimensional models for such a metallic benzene. We also probe the possible first steps in a localized, nucleated benzene polymerization by studying the dimerization of benzene molecules. Several new $(C_6H_6)_2$ dimers are predicted.

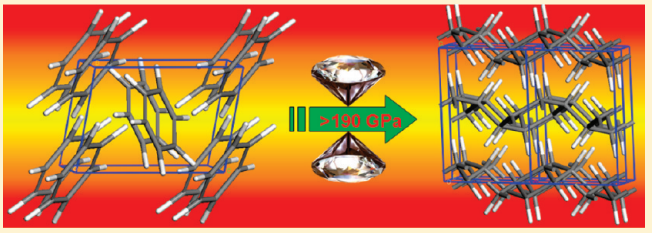

The stable phase of carbon under high pressure (up to 500 GPa) is diamond, a wide band gap insulator.[1] Hydrogen, which has been metalized,[2] does not become metallic under static conditions until P > 350 GPa.[3] Could an "alloy" of C and H be different and metalize at a lower pressure? This is the impetus behind the work reported in what follows.

THE BENZENE PHASE DIAGRAM, AND PREVIOUS STUDIES

Consider an equal carbon−hydrogen ratio, a 1:1 assembly. Among CH systems, benzene (C_6H_6), the emblem of organic chemistry, comes first to mind as a realization. In fact, solid benzene under pressure has been extensively investigated, from P. W. Bridgman's classic pioneering study[4] to the present.

There are two main views of the phase diagram of solid benzene. The first phase diagram of benzene, shown in Figure 1a, was constructed by Thiéry and Léger from Raman and X-ray studies[5] under high pressure. Liquid benzene crystallizes, at room temperature and about 700 bar, in an orthorhombic phase I (*Pbca*). An intermediate phase I′ was suggested from discontinuities in the cell constants of phase I. Phase II ($P4_32_12$) was said to exist between 1.4 and 4 GPa, and phase III is stable between 4 and 11 GPa. The structure of phase III is monoclinic $P2_1/c$, with two molecules per unit cell. Both the I−II and II−III phase transitions are extremely sluggish. Upon increase of pressure, two more phases were suggested by Thiéry and Léger: benzene III′, stable between 11 and 24 GPa, and benzene IV, stable at even higher pressure.

When benzene is compressed above 24 GPa at 25 °C, a solid compound is recovered after the pressure is released. The structure of that solid is not known. Benzene III′ is supposed to be only a modification of benzene III, and benzene IV is thought to be polymer-like. Phases I′, III′, and IV are not well-characterized, and there is still some debate on whether they are established phases or not.

Another phase diagram was developed by Ciabini et al.[6,7] in 2005 from infrared spectroscopy and X-ray analysis under high pressure, shown in Figure 1b. Phase I is orthorhombic *Pbca*. Phase II, crystallizing in space group $P2_1/c$, is the same as phase III assigned by Thiéry and Léger. The $P2_1/c$ phase is stable up to

Received: March 8, 2011
Published: April 27, 2011

   dx.doi.org/10.1021/ja201786y | *J. Am. Chem. Soc.* 2011, 133, 9023–9035

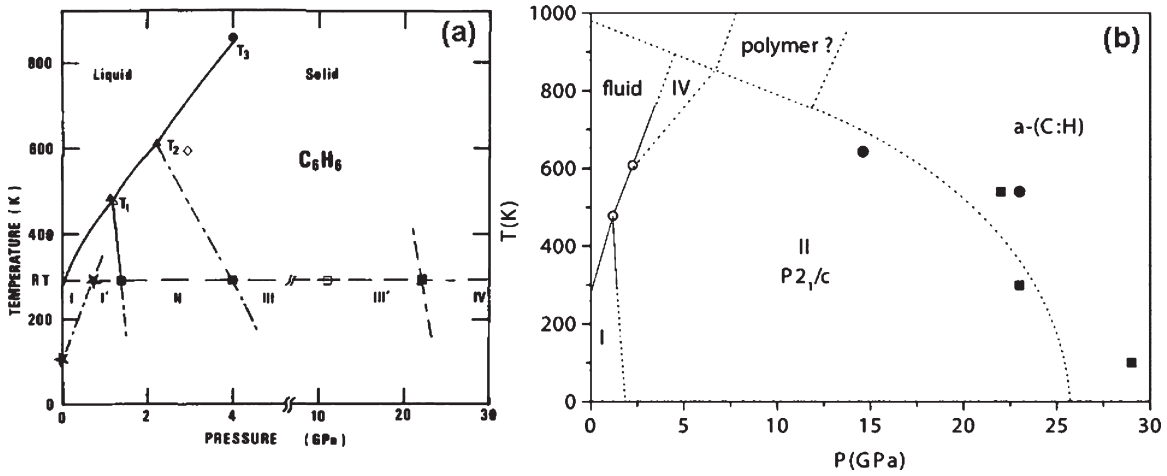

Figure 1. Phase diagrams of benzene: (a) suggested by Thiéry and Léger[5] and (b) proposed by Ciabini et al.[6,7]

pressures of 20−25 GPa, at which point chemical reaction between benzene units is supposed to take place. In this phase diagram, one sees only phases I (*Pbca*) and II ($P2_1/c$), and IV as a possible high-temperature variant of phase II. No indications of II−III and III−III′ phase transitions were found in the work of Ciabini et al. The same research group in 2001 presented results differing from their 2005 measurements; they confirmed then that the transition between phases II and III ($P2_1/c$) is at 4.8 GPa, and the transition from phase III to III′ is at 11.2 GPa. This study also presumed a phase V in the high-temperature region. In their early work, Ciabini et al. used the same notation as Thiéry and Léger.

A reviewer has pointed out to us that the apparent differences between the two phase diagrams are likely the consequences of technical improvements that occurred between the two experiments. Synchrotron-based diffraction experiments and FTIR spectra on both unannealed and annealed samples[6] allowed one to understand the metastability of phase I on pressurizing the sample at room temperature. These results are consistent with those previously reported by Piermarini et al.[8] and recently confirmed by single-crystal diffraction studies by Katrusiak, Podsiadło, and Budzianowski.[9] We thank the reviewer for his or her guidance here.

To summarize, Thiéry and Léger's phase II[5] is not found in subsequent studies, and their phase III (phase II of Ciabini et al.[6,7]) is the only stable one at high pressure.

Theoretically, several high-pressure benzene phases were predicted by Raiteri et al.[10] utilizing a metadynamics method. Seven phases labeled as I, I′, II, III, III′, IV, and V, in the notation used by Thiéry and Léger, were proposed on the basis of this crystal structure prediction method. Phases I (*Pbca*), II ($P4_32_12$), and III ($P2_1/c$) were reproduced by the metadynamics. Phases I′, III′, IV, and V were predicted to crystallize in *Cmca*, *C*2/*c*, *Pbam*, and $P2_1$ space groups, respectively. However, no enthalpy profile as a function of pressure was presented for the phases calculated.

In the present work we study carefully benzene over a range of pressures up to 300 GPa. We provide a possible explanation for the complexities observed in benzene at high pressure, and we pay attention to the electronic properties of benzene phases in the context of our strategy of alloying enhancing metallization.[11−13]

Before beginning the story, we need to mention an essential limitation in what we do, one that limits comparison to experimental reality. We are unable to study effectively amorphous structures. Clearly, benzene under pressure gives rise to amorphous, partially or fully saturated, materials, not that these are well characterized.[14,15] Their formation is clearly nucleated, and a legitimate question is whether the regular benzene or saturated structures (for, as we will see, we find such) are relevant to what is observed. We will return below to the experimental work and the dilemma of interpretation that is a problem for experiment as well as theory here.

THEORETICAL METHODS

The density functional theory (DFT) calculations employed in this paper are based on the plane wave/pseudopotential approach using the computer program VASP (Vienna Ab-initio Simulation Package)[16,17] employing the PBE exchange and the projected-augmented wave (PAW)[18,19] method. The energy cutoff for the plane-wave basis was set to 600 eV. The Brillouin zone was sampled by an automatic mesh of 60 points (converted to Monkhorst−Pack meshes on the basis of the structures' unit cell). Relaxation of the electronic degrees of freedom was stopped when the total (free) energy and the band structure energy changed between two steps by less than 1×10^{-6}. A conjugate-gradient algorithm was used to relax the ions into their instantaneous ground state. We allowed all structural parameters (atomic position, lattice constants) to relax; each structure was reoptimized twice to check reproducibility. All atoms are fully relaxed until the Hellmann−Feynman forces is less than 0.01 eV/Å. The evolutionary algorithms USPEX[20−22] and XtalOpt[23] were employed to find the lowest energy structures.

We might note also that zero-point energies are not included in these calculations; they should be very similar in all the benzene structures considered here, as all of them have the same bonding patterns.

For MD annealing simulation, only the Γ k-point was used, with an energy cutoff of 600 eV. Since the CH stretching motion has a period of 11−12 fs, a 1 fs time step is utilized.

Dynamical stability was checked by phonon calculations carried out using the linear-response method in the Quantum-ESPRESSO code. Pseudopotentials for H and C were also generated by a Troullier−Martins norm-conserving scheme; the structural parameters and electronic structures at both ambient and high pressures obtained with these were comparable with the results obtained from standard VASP pseudopotentials.

There are inherent limitations in this approach, voiced well in the following comment by a reviewer: "[This] model considers one solid phase only and therefore cannot describe genuine thermodynamic transitions between phases of equal free energy. There is a wide literature

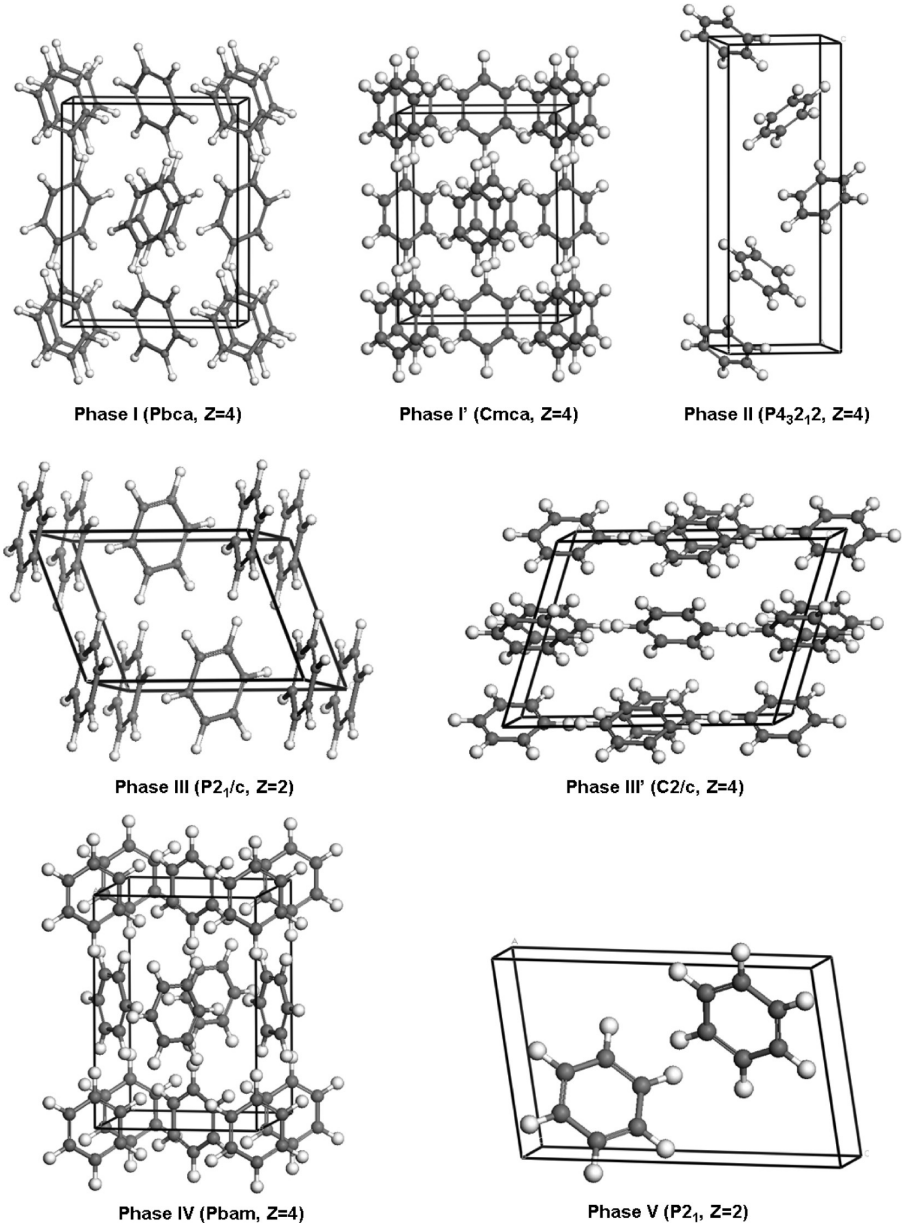

Figure 2. Reoptimized benzene phases at 1 atm. Phases I (*Pbca*), II ($P4_32_12$), and III ($P2_1/c$) were characterized experimentally by Thiéry and Léger.[5] Phases I′ (*Cmca*), III′ (C_2/c), IV (*Pbam*), and V ($P2_1$) were theoretically predicted by Raiteri et al.[10]

on this topic which goes back to Herzfeld and Goeppert Mayer.[24] A correct prediction of a phase transition requires an accurate calculation of the free energy in the two phases, though stability criteria are still useful and true transition pressures are usually not too distant from the calculated values."

RESULTS AND DISCUSSION

Enthalpy of the Benzene Phases as a Function of Pressure. In the gas phase benzene is a D_{6h} molecule with C−C = 1.40 Å and C−H = 1.09 Å. The melting point of benzene is 279 K; the boiling point is 353 K. At normal pressures, one expects a variety of polymorphs to be of roughly equal energy, a typical situation for molecular crystals. Indeed, three phases are well-characterized experimentally: phases I (*Pbca*), II ($P4_32_12$), and III ($P2_1/c$). Our theoretical optimization reproduces the structures of these phases well as far as C−C and C−H distances go, but less well for the unit cell parameters. The details are in the Supporting Information (SI). The calculated C−C and C−H distances match the experimental ones. The unit cell parameters are within 5% of experiment.

Should we have done better or worse on these? The cell parameters are determined essentially by dispersion forces and electrostatic interactions (quadrupole−quadrupole being the leading term for benzene). The DFT method we use is not good at gauging dispersion forces, so the moderately poor agreement with experimental force constants was not unexpected. We are aware that it is possible to apply corrections to get a better accounting of the van der Waals forces.[25−27] We chose not do so because our interest was not so much in the ambient pressure structure as in that at elevated pressure, where such corrections may not be necessary.

dx.doi.org/10.1021/ja201786y | *J. Am. Chem. Soc.* 2011, 133, 9023–9035

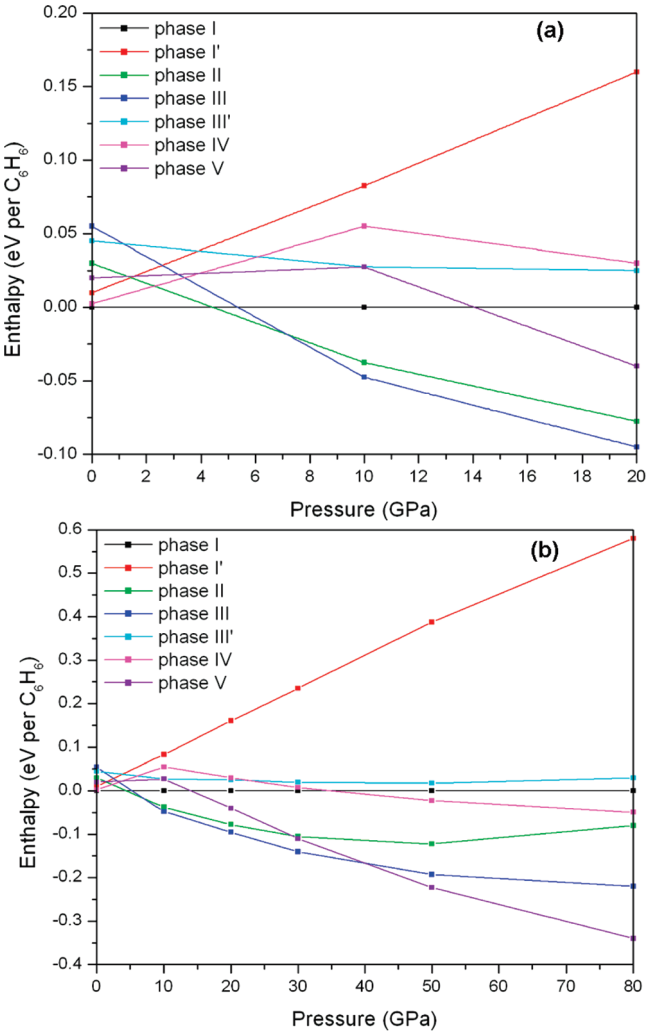

Figure 3. Calculated relative enthalpy curves of benzene phases as a function of pressure in the ranges of (a) 0−20 and (b) 0−80 GPa. Here phase I is taken as a reference.

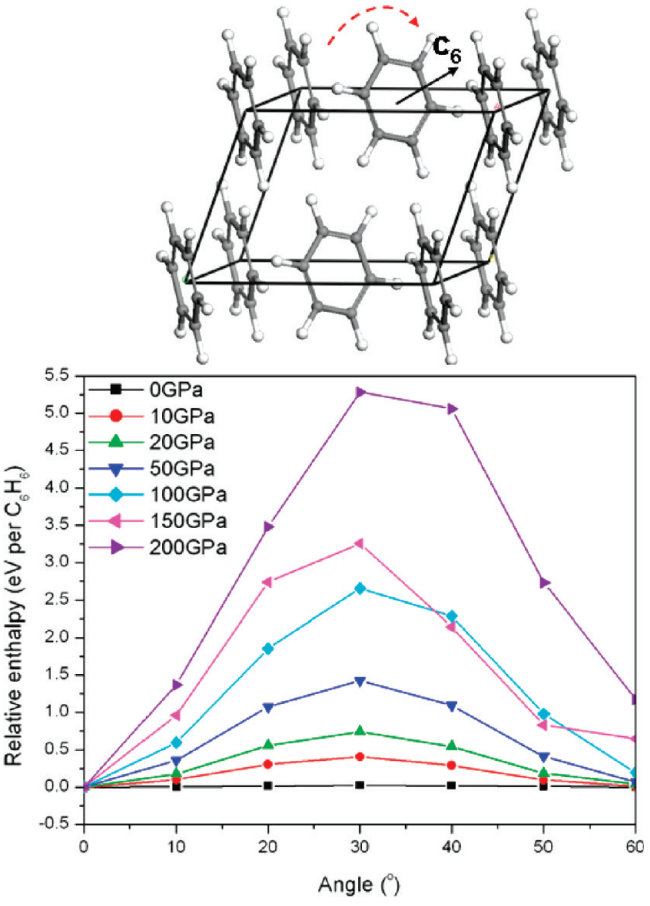

Figure 4. Energy barrier to benzene rotations in phase III structures at various pressures. The "perfect" structure at the corresponding pressure is taken as a reference. Above: definition of the rotation studied.

On elevating pressure, the error in the unit cell parameters is reduced to within 1%, where structural parameters are available (see SI). The lattice parameters of the higher pressure phases remain a matter of controversy. Raiteri et al. predicted the existence of four further phases, phases I′ (*Cmca*), III′ (C_2/c), IV (*Pbam*), and V ($P2_1$).[10] We reoptimized the seven benzene phases mentioned, since our methodology differs somewhat from that of Raiteri et al. Figure 2 shows these optimized benzene phases at 1 atm. The lattice parameters and simulated powder diffractions for these phases also at 1 atm are shown in the SI.

In addition, four more hypothetical benzene models were considered: two known structures of C_6F_6 and C_6F_6−C_6H_6 and two phases with parallel benzene molecules. These phases are not competitive with the most stable phases III and V, as shown in the enthalpy curves in the SI.

We proceeded to optimize the structures of these seven phases over a wide range of pressures. Figure 3 shows the enthalpy curves of the benzene phases as a function of pressure in the ranges of 0−20 and 0−80 GPa. At 1 atm, the enthalpy differences among the seven benzene phases are tiny; these structures are within 0.05 eV per benzene molecule of each other. Nothing surprising here—there clearly are many ways for anisotropic dispersion forces to hold benzene molecules together in a molecular crystal. The structures become differentiated in enthalpy as the pressure increases.

From Figure 3, we can see that, at least theoretically, the phase I → phase II transition should occur at ∼4 GPa, phase II → phase III at ∼7 GPa, and phase III→ phase V at ∼40 GPa. Above 40 GPa, phase V comes into play and proceeds to become the most stable structure at still higher pressures. Phases I′, III′, and IV suggested by Raiteri et al. are not competitive with phases I, II, III, and V by our calculations in the whole pressure range studied. Experimentally, both the I−II and II−III phase transitions are extremely sluggish, phase II existing between 1.4 and 4 GPa, and phase III existing between 4 and 11 GPa. The current computation agrees reasonably well with the order of phase transitions found in experimental studies in the low and moderate pressure regime.

Might the benzene structures we calculate be rotational solids, as solid H_2,[28] solid CH_4,[29] and the C_{60} crystal structure[30] are? Let us probe this with a numerical experiment. Consider phase III, which has two benzene molecules in the unit. We rotate one of the benzene molecules along its C_6 axis while another benzene molecule is frozen. Other rotations encounter large barriers. Figure 4 shows the energetic consequences of this rotational motion as a function of pressure.

At 1 atm, this benzene rotation is free as it is in methane. As expected, the rotational barrier is elevated with increasing

dx.doi.org/10.1021/ja201786y |*J. Am. Chem. Soc.* 2011, 133, 9023–9035

pressure. It is not clear what barrier might be considered a cutoff for labeling a material as a rotational solid. If we choose a barrier of less than 0.5 eV, then only at pressures below 20 GPa would the rotational solid description be warranted.

Phase Transformations Rear Their Heads. To provide some focus for our studies, we concentrate from this point on phases III and V, whose enthalpy is shown over a still wider enthalpy range in Figure 5. Note that we have switched from relative enthalpy to absolute; this makes it easier to spot phase transitions.

Given the computed stability of phase V at pressures >40 GPa, we examined this phase first. Phase V evolves from $P2_1$ at ambient pressure to $P2_1/c$ at elevated pressure. Above 80 GPa, phase V spontaneously undergoes in our calculations a pressure-induced chemical transformation to a curious polymeric phase we have labeled "polymer I". The discontinuity is apparent in Figure 5. Figure 6 shows two views of polymer I at 100 GPa. One sees in this structure one-dimensional arrays, with all carbons tetracoordinate. These CH needles or tubes contain five-, six-, and eight-membered rings. They could be thought of as one-dimensional arrays of C_6H_6 rings bridged to each other by three

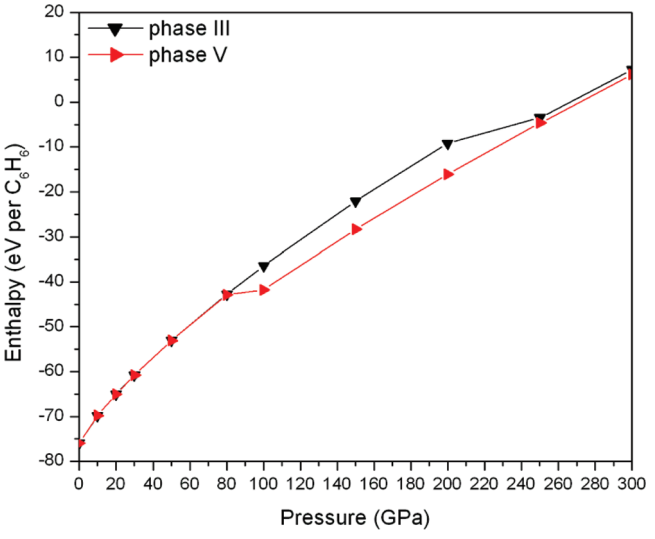

Figure 5. Calculated absolute enthalpy curve of benzene for phases III and V as a function of pressure (up to 300 GPa).

σ bonds on one side and three on the other. The C−C distances are in the range of 1.42−1.57 Å. The closest H···H distance between the CH tubes is 1.56 Å. The calculated band gap of polymer I at 100 GPa is around 5 eV (see SI), indicating that polymer I should be transparent. This is not surprising, given the four-coordinate C structure. The gap remains at higher pressures.

We began to wonder if this transformation could occur at a lower pressure. First, we extended the pressure "backward" on polymer I, studying it a pressures lower than 80 GPa. The tetracoordinate, saturated structure is dynamically stable, as determined by a phonon analysis, and at all pressures is more stable than phase V!

We then looked at the dynamic stability of molecular phase V gauged by phonon calculations, now at lower pressures. At 10, 20, and 50 GPa, phase V is dynamically *unstable*. Following the imaginary frequencies of vibration, one comes again to polymer I.

This four-connected CH structure is the harbinger of what is to come—*"saturated", four-connected carbon structures must be considered for benzene under pressure*, for they are often more stable than molecular analogues. No claim of novelty here—Nicol and Yin entitled a 1984 paper, "Organic Chemistry at High Pressure: Can Unsaturated Bonds Survive 10 GPa?"[31,32] One had better also worry about kinetics, set by the barriers between structures.

We return to phase III, the most stable molecular phase calculated for benzene in the pressure range of 7−40 GPa, as Figure 3b shows. This phase remains molecular up to much higher pressures than any other benzene phase. Phonon dispersion calculations show that phase III is dynamically stable up to 190 GPa; for phase III a pressure-induced chemical transformation, without thermal activation, occurs only above ∼200 GPa.

The phase transformation that does occur in phase III at ∼200 GPa is a drastic one. Above this pressure we find polymer II, whose structure is shown in Figure 7. Polymer II is a stacking of CH sheets containing four-, six-, and eight-membered carbon rings bonded with H atoms on both sides. All carbons in this structure are four-coordinate. The C−C distances are in the range of 1.36−1.43 Å at 210 GPa; for calibration the C−C distance in diamond at 210 GPa is 1.412 Å, so the polymer II distances are normal. The original six-membered rings are actually discernible in the polymer structure—one way to describe the two-dimensional network is as the product of a

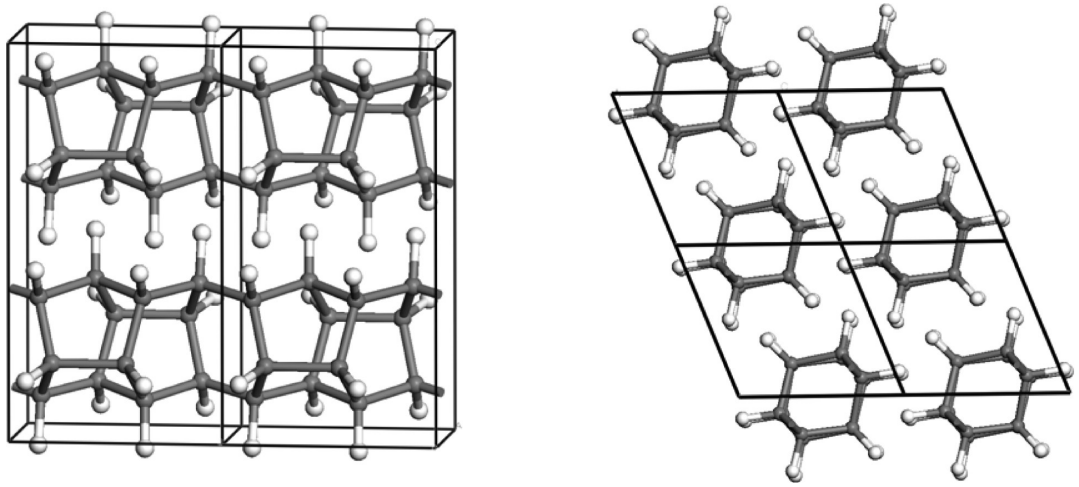

Figure 6. Two views of polymer I at 100 GPa. On the left is a side view, on the right a top one.

dx.doi.org/10.1021/ja201786y |*J. Am. Chem. Soc.* 2011, 133, 9023–9035

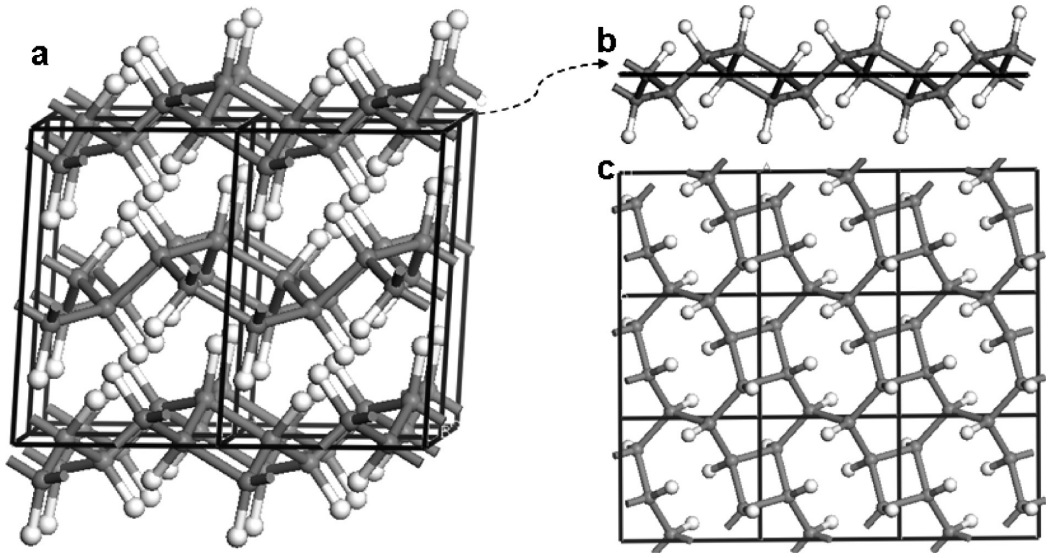

Figure 7. Different views of polymer II at 210 GPa: (a) 3D structure of polymer II, (b) side view of a single layer in polymer I, and (c) top view of the single layer.

Scheme 1. Schematic Formation of a Four-Coordinate C Polymer from Benzene[a]

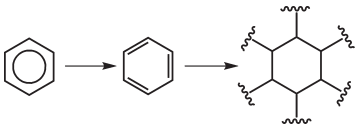

[a] Hydrogens are omitted from this portrayal.

(formally forbidden) 2+2 dimerization of a chain of benzenes, along with a 1,4-polymerization to give a sheet.

Saturated CH Polymers Are More Stable than Benzene Phases. At this point we have an interesting mystery before us—two (so far) polymeric four-coordinate structures, polymers I and II, are more stable than any benzene structure. To an organic chemist, used to the archetype of benzene, this is a surprise. It should not be.

Let us construct a way to think of this problem, sketched in Scheme 1. In the first step in a *Gedankenexperiment*, the benzene is "dearomatized"; in the second step, the resulting cyclohexatriene converts to a saturated polymer.

There is a range of values of the energetic value of aromaticity. Following Shaik and co-workers,[33] we use the larger value in the literature, a so-called "vertical" resonance energy, ~65 kcal/mol, to create from benzene a cyclohexatriene with all aromaticity removed. To reach one of the saturated CH polymorphs from such a "dearomatized" cyclohexatriene involves the further conversion of three C=C bonds to three σ C−C bonds inside the benzene hexagon, and three more σ C−C bonds outside, as sketched in Scheme 1.

The second (π) bond of any double bond is energetically worth less than a single bond. This is not a number one can measure directly. One estimate of the preference comes from the heat of reaction of three ethylenes (C_2H_4) to cyclohexane (C_6H_{12}), a process in which in fact three π bonds are converted to three σ bonds (see Scheme 2). That heat is experimentally −67 kcal/mol.[34]

Scheme 2. Reaction of Three Ethylenes to Cyclohexene: A Model for Three C=C Bonds Converting to Six C−C Bonds

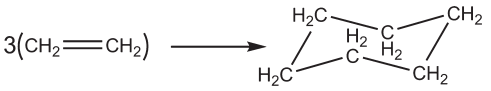

Another way to estimate the energy of breaking a π bond is to look at the energy of rotating the two CH_2 groups in ethylene 90° out-of-plane (~65 kcal/mol[35]), and to compare that to a CC σ bond strength (~90 kcal/mol[36]). That would lead to a slightly larger estimate of −75 kcal/mol for three bonds.

The sum of the two heats for processes A and B is 65 − 67 (or − 75) = −2 (or −8) kcal/mol C_6H_6. We will see that this is not a bad estimate.

Graphanes. The needle-like structures of polymer I and the sheets of polymer II contain four-, five-, and eight-membered rings. One can do better in the organic chemistry of saturated systems (which is what we have before us) so far as angle strain is concerned. We therefore began at this point to look at graphanes, CH sheets with all six-membered rings.

Graphane is a fully saturated CH hydrocarbon conceptually derived from a single graphene sheet. This structure was first computed in 2003 by Sluiter and Kawazoe,[37] and in 2007 by Sofo et al.,[38] and synthesized in an approach to a pure form in 2009 by Elias et al.[39] (see also the earlier work from the Brus group[40]). Our work on the system is described in detail elsewhere.[41] There are actually many isomeric single-sheet graphanes (see the enumeration in refs 18 and 22); the four we have found that are more stable than benzene are shown in Figure 8.

Two of these sheets may be derived by taking single-layer slices from the cubic diamond structure, three from hexagonal diamond. Sheet B also occurs (not for carbon) in many inorganic compounds, such as $BaIn_2$,[42] TiNiSi,[43] or EuAuSn,[44] as a planar motif in a three-dimensional structure. The all-chair sheet A and boat sheet C have forerunners in the CF literature;[45−47] sheets B and D have also been suggested for CH by others.[48,49] In our own work[41] we have also come on some new sheets, but none so stable as the four shown.

dx.doi.org/10.1021/ja201786y | J. Am. Chem. Soc. 2011, 133, 9023–9035

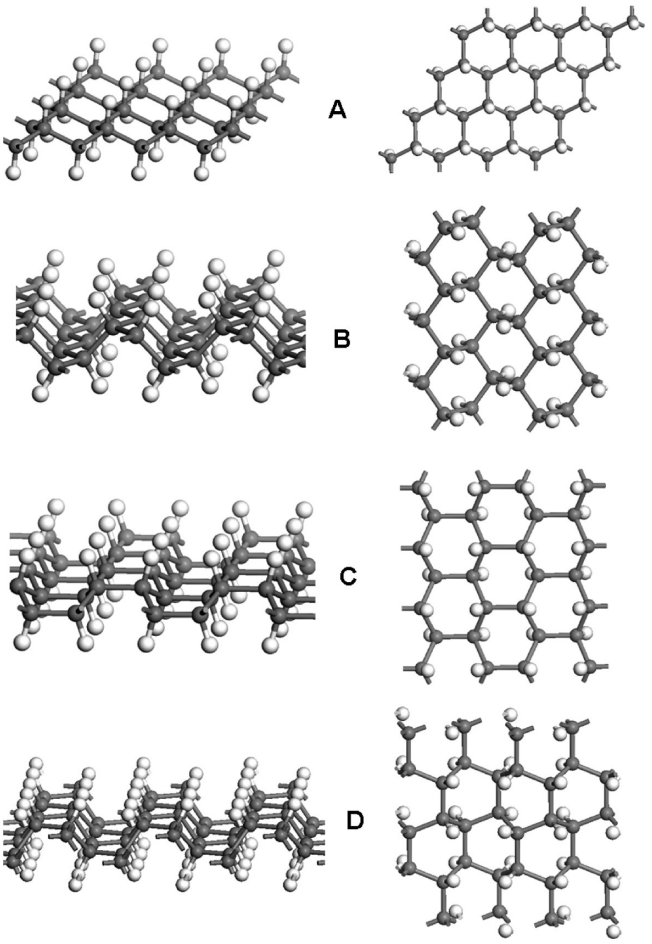

Figure 8. Four isomeric single-sheet graphanes. Side views are at left, top views at right.

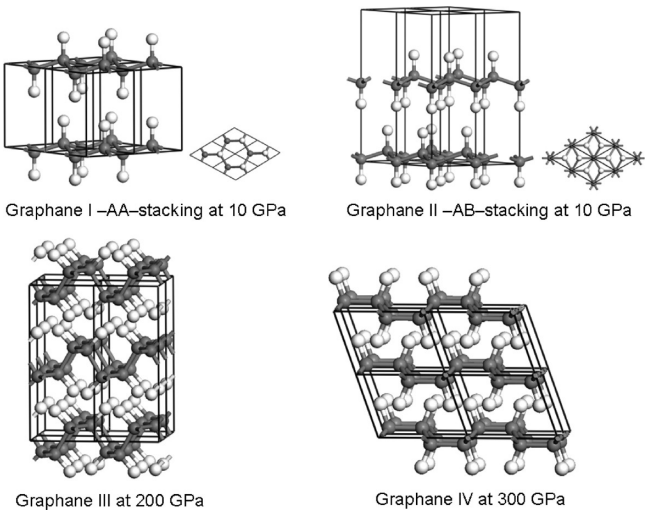

Figure 9. Graphane I (at 10 GPa), II (at 10 GPa), III (at 200 GPa), and IV (at 300 GPa) structures.

On packing these layers in three dimensions, one can obtain a number of polytypes. Figure 9 shows four of these; others may be found in our detailed study.[41] We first found these structures (except for graphane I) by using an evolutionary algorithm

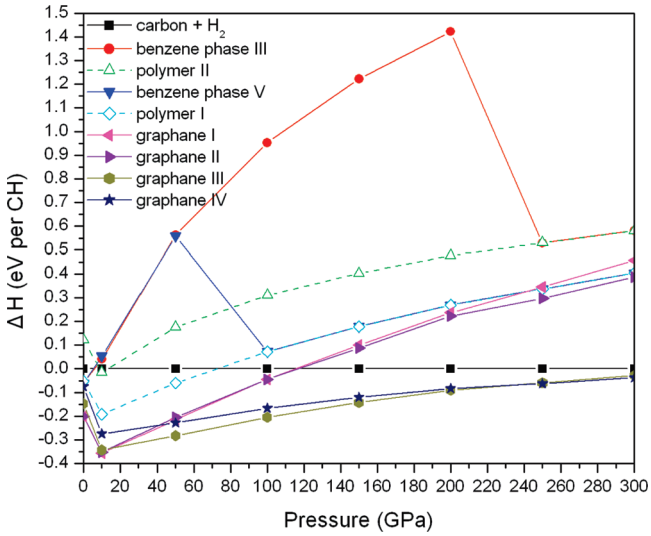

Figure 10. Enthalpy of various CH systems as a function of pressure. The reference is the most stable phase of carbon and H_2: graphite below 10 GPa and cubic diamond above 10 GPa; for H_2, $P6_3/m$ (<100 GPa), $C2/c$ (100−250 GPa), and *Cmca*-12 (>300 GPa). Note that zero-point energies are not included in these calculations.

structure search (USPEX) at one pressure. The structures so obtained were then taken over a wide pressure range.

Figure 10 shows the static lattice enthalpies of various CH systems, including benzene phase III, benzene phase V, the two polymeric structures mentioned earlier, and the graphane-type phases obtained by us using the evolutionary algorithm search. The corresponding most stable carbon (graphite below 10 GPa and cubic diamond above 10 GPa) and H_2 phases[50] are taken as references. The graphite-to-diamond phase transition around 10 GPa causes the apparent kink in the graphane relative enthalpy curves at that pressure; there is no discontinuity in their intrinsic enthalpy curves.

For the CH system, the most stable phase we found in the range 0−10 GPa is the all-chair graphane -AA- stacking or -AB-stacking, both dynamically stable (see SI). These phases are close in energy over a wide pressure range. Graphane III becomes the most stable phase in the range of 10−200 GPa. The calculated phonon dispersion for both graphanes III and IV shows no imaginary frequencies at 200 and 300 GPa, indicating that both are dynamically stable. The reasons for the increasing stabilization of graphanes III and IV with pressure (relative to I and II) are discussed elsewhere; the differential can be traced to the balance of inter- and intrasheet H···H interactions.[41]

Graphanes I and II should interconvert easily, for what is involved is merely the sliding of layers. But the interconversion between this pair and graphane III or IV should be difficult—many CC bonds would have to break in the process. These are geometrical isomers, not conformers.

So why do the benzene phases (III and V) not convert spontaneously to these four-connected polymers? Because there are likely significant barriers to polymerization. Organic chemistry as a whole is an exercise in kinetic persistence. The isomers of benzene itself (Figure 11) are but one example of this. So prismane, benzvalene, and Dewar benzene are respectively no less than 114, 81, and 80 kcal/mol less stable than benzene. However, they were made in the 1960s and 1970s;[51−53] despite slow decomposition to benzene, they have a half-life long enough

dx.doi.org/10.1021/ja201786y |*J. Am. Chem. Soc.* 2011, 133, 9023–9035

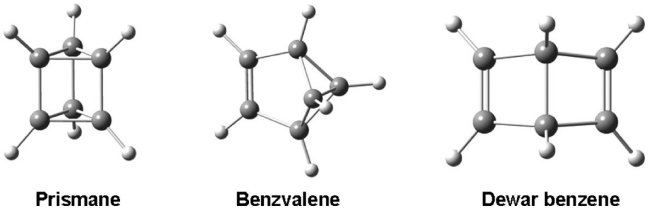

Figure 11. Three known isomers of benzene.

to allow isolation. The reversions of these to benzene are forbidden reactions.[54]

To summarize: at every pressure studied, saturated, four-coordinate CH phases, and graphanes in particular, are more stable than any phase retaining discrete benzene molecules. Furthermore, the transformation from benzene to saturated hydrocarbon may well be local or nucleated. The outcome would be an amorphous, approximately four-coordinated polymer. We will return to the first stages of nucleated polymerization later in this paper. It seems to us likely that such polymers, difficult if not impossible to calculate, are in fact the experimentally observed polymeric products of the pressurization of benzene.

DFT computations apply to the $T = 0$ K and static situation. To analyze the effect of temperature on benzene phase III, we performed an annealing simulation using the ab initio molecular dynamics (MD) method.[55] For the annealing process, the initial temperature of the system is increased to 300 K, and a final temperature of 0 K is requested. The annealing analysis indicates that the chemical transformation (to a saturated polymer) occurs in phase III when the pressure is above 150 GPa at elevated temperature. If the temperature is higher still, the transformation may occur at a still lower pressure.

Ciabini et al.[7] used MD simulations to study several amorphization events in benzene from configurations equilibrated (phase III) at 23 GPa and 540 K. All the reactive events are irreversibly initiated when the nearest-neighbor (nonbonded) C···C distance approaches 2.5−2.6 Å. In our case, the nearest-neighbor C···C distance in phase III at 190 GPa and 0 K is 2.4 Å, which is similar to the distance at 23 GPa and 540 K obtained by Ciabini et al. In fact, Ciabini et al. did not observe any reaction in a pressure range up to 150 GPa—only an increase of the atomic kinetic energy (up to 1500 K at 23 GPa) was able to induce the amorphization in a few hundred femtoseconds. This indicates, as suspected, that temperature is also an important factor in the phase transitions of benzene. Note that there is a difference in the structures obtained by Ciabini et al. and us: our polymer II is an ordered crystal structure and not amorphous. The length of the simulation and the temperature may be responsible for the difference.

Does this mean that we should desist and not study the effect of pressure on benzene? Not at all. As our calculations also show, the various benzene phases are local minima, dynamically stable over a wide pressure range. They will face substantial barriers to transforming into graphanes. Phase III in particular is a benzene structure that in our calculations is persistent to ∼200 GPa at 0 K. Thus, it makes sense to inquire into the properties of the most persistent benzene phases, such as phase III, focusing on their eventual metallization.

Approaches to Metalization while Maintaining a Benzene Structure. As we saw earlier in our calculations, benzene remains in phase III until ∼200 GPa at $T = 0$ K, despite saturated phases being more stable. At ∼200 GPa it transforms spontaneously to a polymeric saturated CH phase. As phase III is compressed, the band gap becomes smaller, and at ∼180 GPa it vanishes, within the tolerances of the GGA computational approach we use. This region, 180−200 GPa, in which one has a metallic benzene phase that has a barrier to rearrangement to a saturated polymer, is of substantial interest to us. We next describe in some detail the approach to metallization.

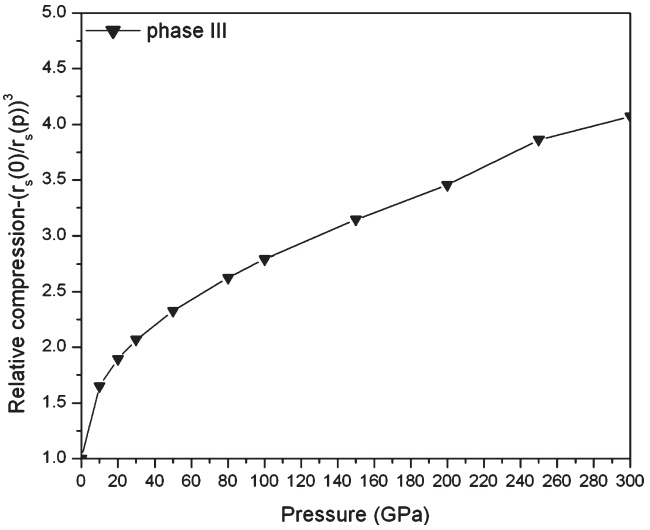

Figure 12. Computed relative compression as a function of pressure in benzene phase III. The relative compression is defined by $[r_s(0)/r_s(p)]^3$, where $r_s(0)$ and $r_s(p)$ are the Wigner−Seitz radius at ambient pressure and calculated high pressure, respectively.

Figure 12 shows the computed relative compressions of benzene phase III as a function of pressure. The Wigner−Seitz radius r_s is defined by $4\pi r_s^3/3 = 1/\rho$, where ρ is the average valence-electron density. Since $\rho = N/V$, where N is the number of valence electrons in the unit cell and V is the volume of the unit cell, ρ scales as $V^{-1/3}$. The volume reduction for all the benzene phases, not only phase III, is rapid between 0 and 10 GPa and is attributable to the squeezing out of the van der Waals space between benzene units. Such behavior has been observed in many molecular crystals under pressure.[56,57]

The remarkably useful Goldhammer−Herzfeld criterion for metallization[58] holds that an insulator or semiconductor is likely to become a metal when the conditions on the density are such that the bulk polarizability diverges; that is, electrons can be stripped off the atoms or molecules with a diverging local field associated with an infinitesimal perturbation. To be specific, the Goldhammer−Herzfeld criterion says that a material becomes metallic when the quantity $(1 - f\alpha V_m)^{-1}$ diverges, where α is the molecular polarizability, V_m the volume per molecule in the solid, and f a dimensionless factor determined only by the packing of the molecules in the crystal. The divergence occurs when $f\alpha/V_m = 1$. For cubic systems $f = 4\pi/3$, and this gives $V_m = 4\pi\alpha/3$. Using the definition of r_s, $4\pi r_s^3/3 = V_m/N_{ve}$ (where N_{ve} is the number of electrons), we then have the following condition for cubic systems, namely $r_s = (\alpha/N_{ve})^{1/3}$. The average polarizability of benzene, α, is 67.55 bohr;[3] $N_{ve} = 30$ in one benzene molecule. One then gets $r_s = 1.31$ for the metallization of benzene.

The real benzene structure (phase III is under discussion) is, of course, not cubic. Still the arguments made above carry over well—as Figure 13 shows, the band gap goes to zero at $P \approx 180$ GPa, where $r_s = 1.31$ and the relative compression is just around 3.0.

dx.doi.org/10.1021/ja201786y |J. Am. Chem. Soc. 2011, 133, 9023–9035

Figure 14 shows the calculated total density of states (TDOS) and Fermi surface for benzene phase III at 190 GPa, a pressure at which it is metallic yet, at 0 K, still stable with respect to rearrangement to a saturated polymer. The underlying band structure is shown in the SI. Note the TDOS shows a characteristic free-electron-like shape over a wide energy range. As we noted earlier, above $P = 210$ GPa, phase III undergoes a pressure-induced chemical transformation to polymer II. Once a saturated molecule is achieved, the band gap opens up again—polymer II and the graphanes have large band gaps. Based on the band gaps in phase III (Figure 13), we suggest that, upon increasing pressure, benzene will turn from transparent to colored to black and then colorless again as it polymerizes.

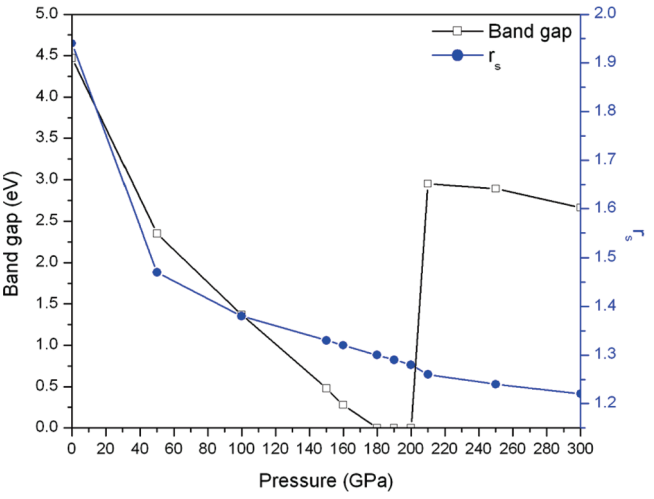

Figure 13. Relationship among band gap (in eV), pressure, and Wigner–Seitz radius (r_s).

Could there exist a "Kekulé metal" in benzene in the (narrow) pressure range where it is calculated to be metallic? The speculative notion here is of a Kekulé state of the π systems for each molecule, delocalized yet contained in a six-membered carbon ring, that might then be phase-linked via the bridging hydrogens, a Bloch-like state being the consequence. If so, then this could be a realization of the resonant valence bond state proposed by P. W. Anderson as a possible basis for high-temperature superconductivity[59] (pairing via Kekulé states in a "Kekulé metal", one might optimistically say).

Another way to follow the approach to metallicity of a material is via its dielectric function. The probability of photon absorption is also directly related to the imaginary part of the optical dielectric function $\varepsilon(\omega)$. In the SI we show the computed dielectric functions of phase III at 0, 190, 200, and 210 GPa. These calculations indicate—through Drude behavior at low frequencies—that the structure at 0 GPa (molecular crystal) and that at 210 GPa (CH saturated polymer) is an insulator, while at 190 and 200 GPa, the dielectric response is characteristic of a metal, as we already concluded from the band gaps.

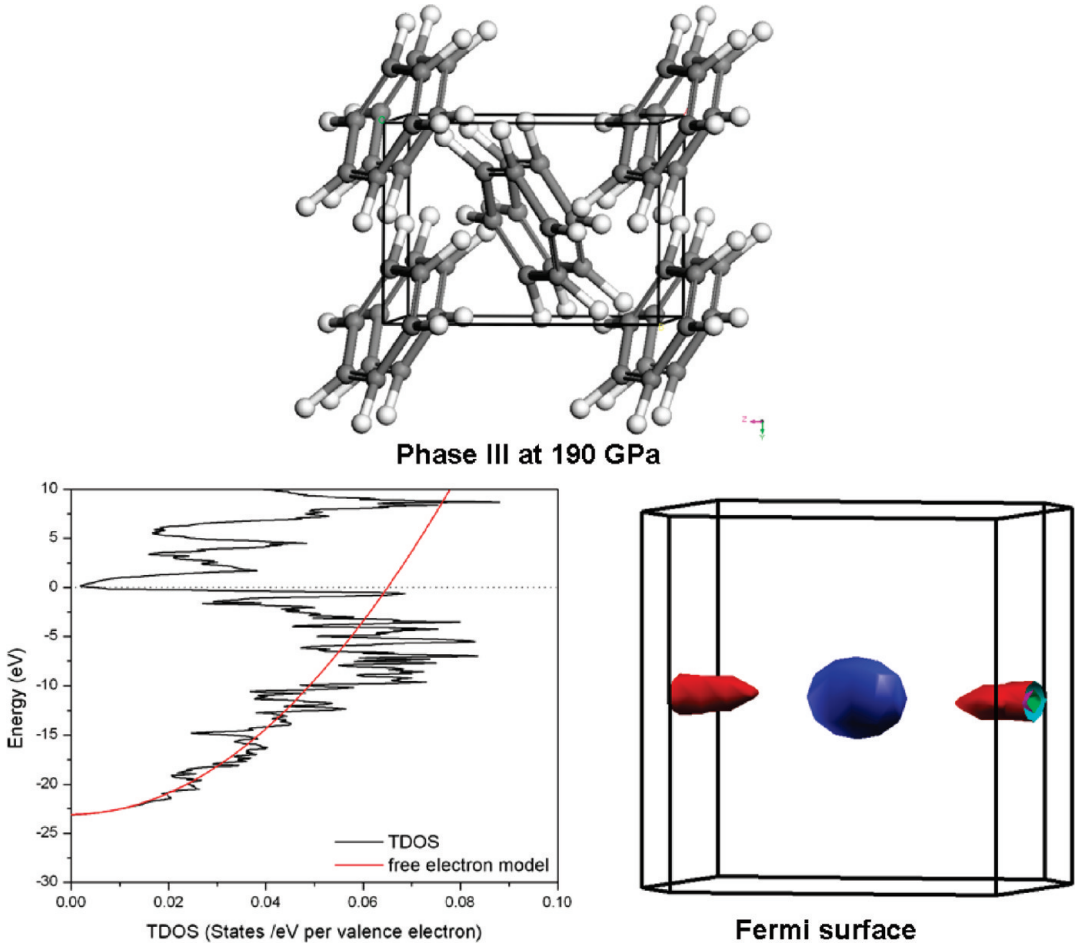

Figure 14. Calculated TDOS and Fermi surface of phase III at 190 GPa.

dx.doi.org/10.1021/ja201786y |*J. Am. Chem. Soc.* 2011, 133, 9023–9035

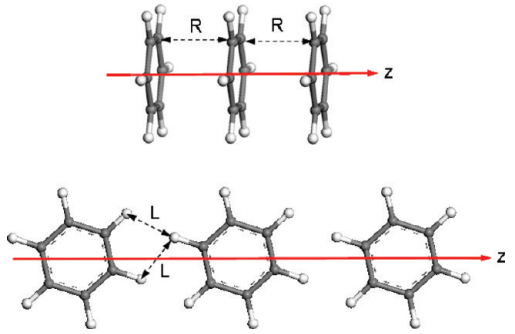

Figure 15. (Top) Stack of benzenes, a model for π interaction. (Bottom) One-dimensional benzene array, a model for σ interaction.

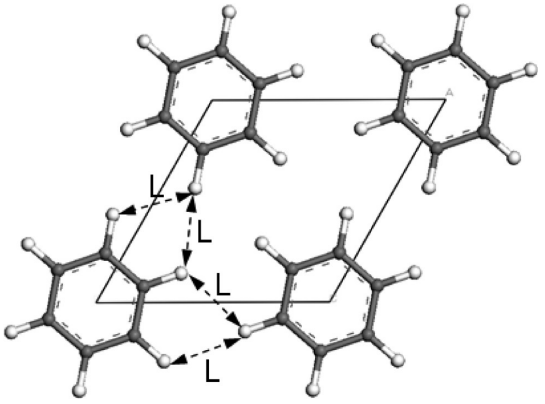

Figure 16. Model of 2D benzene.

Some Model Structures. Some lower-dimensional models are also useful in getting an understanding of the factors governing benzene metallization. Consider first π stacking, as shown in a one-dimensional array in Figure 15 (top). In the process of compressing, the C−C and C−H distances in benzene are frozen. Only the distance between benzene molecules is allowed to vary. This one-dimensional array becomes metallic at $R < 2.5$ Å, due to overlap of π and π^* bands. The situation is similar to a previously studied stack of ethylenes.[60]

Metallization can also be attained by σ overlap of C−H bonding and antibonding orbitals, if the benzenes are so disposed as to emphasize σ interactions. The one-dimensional array shown in the bottom of Figure 15 is one way to do this. This becomes a metal at a center-to-center ring distance of 4.5 Å, at which point the shortest H···H contact $L = 1.25$ Å.

We also calculated a two-dimensional array shown in Figure 16, designed to create equalized H···H contact, L, in a net. When this is compressed, it becomes metallic when the closest H---H contact $L = 1.35$ Å.

We had an idea that in the region of metallization, there might be some unusual dynamics, separating the scale of mobility of C and H atoms. To be specific, we wondered if the carbon rings might move independently of the hydrogens or, alternatively, if the hydrogens would move with relative ease if the carbon atom positions were frozen. This was probed at geometries corresponding to L values above and below the metallization threshold (see SI). However, these motions proved very costly in energy.

Calculated Bulk and Shear Moduli. The stiffness of materials may be measured in a number of ways. Young's modulus (E) describes the material's response to linear strain (like pulling on the ends of a wire). The bulk modulus (K) describes the response to uniform pressure, and the shear modulus (G) describes the material's response

Table 1. Calculated Bulk Modulus, Shear Modulus, and Young's Modulus (All in GPa) for Phase III at a Series of Pressures

		pressure (GPa)				
phase III		50	100	150	190	210
bulk modulus		182	375	450	523	745
shear modulus		68	163	146	99	338
Young's modulus	X	232	422	608	629	1052
	Y	126	397	283	346	1081
	Z	100	335	338	426	652

The calculated bulk modulus, shear modulus, and Young's modulus of phase III at a series of pressures are listed in Table 1. The Reuss definition is utilized to calculate the bulk modulus and shear modulus.[61] The bulk and Young's moduli rise with increasing pressure. At 150 GPa, the bulk modulus of phase III is 450 GPa, which is lower than the value of diamond at that pressure (computed as 850 GPa; as a calibration we calculated the $P = 1$ atm bulk modulus of diamond as 450 GPa, experimental value 443 GPa[62]). At 210 GPa, the computed bulk modulus (745 GPa) of polymer II is also lower than the theoretical value of diamond at this pressure (1100 GPa). Therefore, it should be possible to compress benzene in diamond anvil cells.

Primary Local Actions in Benzene under Pressure. Theoreticians, attracted by symmetry, would like to see all solid-state transformations happen in a concerted manner, preserving as much symmetry as possible at every place in a macroscopic crystal. In the real world, given unavoidable pressure and temperature inhomogeneities, if there is a driving force, chemical and physical transformations are likely to be nucleated, and hence to occur locally. Given a multitude of such local reaction nuclei, the result will likely be an amorphous polymer which is difficult to handle theoretically.

We have seen very clearly that ordered all-saturated, four-coordinate carbon polymers (graphanes and the related needles and sheets) are favored thermodynamically over delocalized, conjugated, three-coordinate polymers (graphite) and molecular structures (benzene crystals) at all pressures. A simple argument showed that converting a double bond to two single bonds is favored. As an approach to the nucleated, local amorphous polymerization problem, we have looked at the dimerization of benzene in some detail. We need to mention here the prior work of Engelke on this subject.[63,64]

To jump-start the process of dimerization, we brought two benzene molecules to an uncomfortably close contact and then let a molecular (zero-dimensional) geometry optimization program complete the optimization. The molecules either moved apart or dimerized. This procedure generated many, but not all, of the known dimers of benzene, as well as some dimers that were really unexpected. We followed this brute-force process with a detailed exploration, including missed known structures and exploring the complete set of stereochemical possibilities for $(C_6H_6)_2$ molecules.

A detailed account of this section of the work will be published elsewhere,[65] as it is of substantive chemical interest—we generated

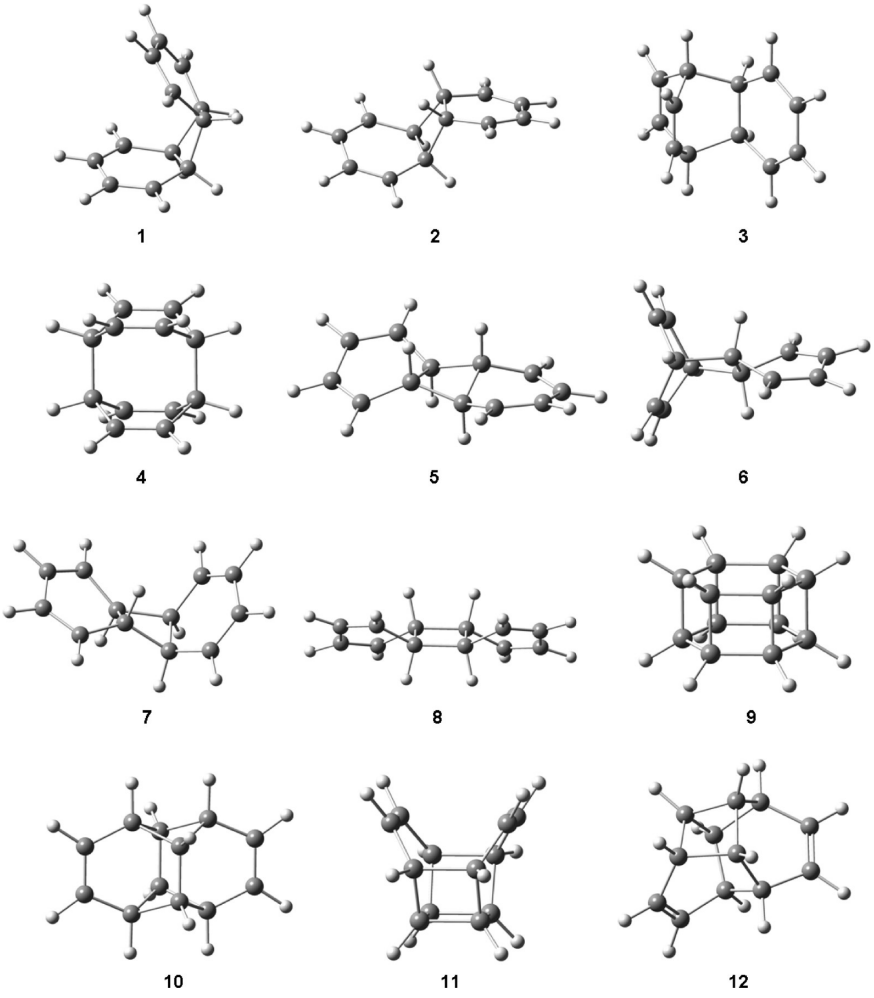

Figure 17. Structures of some benzene dimers.

theoretically some dimers of benzene not yet known and, as we will show, molecules that should be kinetically persistent. Here, in Figure 17, we show just the set of dimers that emerge from this investigation, all local minima on the $C_{12}H_{12}$ surface. Of these molecules, **1**,[66] **2**,[67] **3**,[68] **11**,[69] and **12**[70] are known, as well as derivatives of **4**.[71]

These molecules lie (calculated) 36 (**3**)−112 (**9**) kcal/mol above two benzene molecules. We will give a full account elsewhere[65] of the calculated barriers to the reversion of these dimers to two benzenes, as well as other potential escape routes from their high-energy situation. For the moment, it suffices to say that, for some of the unknown isomers, activation barriers are likely to be high, and these structures have a very good chance of kinetic persistence, even at room temperature. One approach to simulating irregular polymerization of benzene would be to take this set of dimers and proceed with adding a third and a fourth molecule of benzene. That remains to be done.

CONCLUSION

In this study benzene has been compressed in a sequence of calculations up to 300 GPa. The computational results show that the phase I → phase II transition occurs at ∼4 GPa, phase II → phase III at ∼7 GPa, and phase III→ phase V at ∼40 GPa. The agreement with the order of phase transitions found in experimental studies, especially below 10 GPa, is good. Above 50 GPa, hints that molecular structures are unstable with respect to saturated, four-coordinate at C phases—one-, two-, and three-dimensional—led us to examine such phases in detail.

We have found that several graphane phases are more stable than any of the molecular phases over the entire range of pressures studied, including $P = 1$ atm. A qualitative argument for that order of stability is given.

But the molecular phases encounter large—sometimes very large—barriers to rearrangement to a saturated polymer or network of the graphane type. In particular, phonon dispersion calculations show that phase III is dynamically stable up to ∼200 GPa and might become metallic before transformation to a saturated phase. Several simple models for the metallization of benzene are investigated. We also speculate on the possible existence of a phase-coherent Kekulé metal. Finally, in a first approach to nucleated benzene polymerization, we calculate the structures of a number of benzene dimers, some known, some not.

ASSOCIATED CONTENT

Supporting Information. Details of computed benzene phase structural parameters; simulated X-ray diffraction patterns of benzene phases; "parallel" phase I and II, "C_6F_6"

phase, and "$C_6H_6-C_6F_6$" phases; distance histogram and density of states of polymer I; dynamical analysis for phase III; distance histogram of phase III at various pressures; C−C, C−H, intermolecular H---H, and intramolecular H---H distances in phase III; band structure of phase III at 190 GPa; density of states of polymer II at 210, 250, and 300 GPa; computed total density of states for phase III at 190 and 200 GPa, comparing DFT and eH methods; analysis of the lattice stability of phase III at 190 and 200 GPa; effect of rotation on metallization of phase III at 150 GPa; calculated dielectric functions for phase III; phonon dispersion of graphanes; computed total density of states for graphanes; band structure of 1D and 2D benzene models; and three kinds of rotations in 2D benzene models. This material is available free of charge via the Internet at http://pubs.acs.org.

AUTHOR INFORMATION

Corresponding Author

rh34@cornell.edu

Present Addresses

[†]Theoretical Division, Los Alamos National Laboratory, Los Alamos, NM 87545

ACKNOWLEDGMENT

The four reviews we obtained of this paper were extraordinarily detailed and useful—we really appreciate the reviewers' comments. We are grateful to Dr. P. Raiteri for suggesting some benzene phases. Our work at Cornell was supported by the National Science Foundation through Grants CHE-0613306, CHE-0910623, and DMR-0907425, and by EFree, an Energy Frontier Research Center funded by the U.S. Department of Energy, Office of Science, Office of Basic Energy Sciences, under Award Number DESC0001057. This research was also supported by the National Science Foundation through TeraGrid resources provided by NCSA. Some calculations were performed in part at the Cornell NanoScale Facility, a member of the National Nanotechnology Infrastructure Network, which is supported by the National Science Foundation.

REFERENCES

(1) Mujica, A.; Rubio, A.; Muñoz, A.; Needs, R. J. *Rev. Mod. Phys.* **2003**, *75*, 863–912.
(2) Weir, S. T.; Mitchell, A. C.; Nellis, W. J. *Phys. Rev. Lett.* **1996**, *76*, 1860–1863.
(3) Narayana, C.; Luo, H.; Orloff, J.; Euoff, A. L. *Nature* **1998**, *393*, 46–49.
(4) Bridgman, P. W. *Phys. Rev.* **1914**, *3*, 153–203.
(5) Thiéry, M. M.; Léger, J. M. *J. Chem. Phys.* **1988**, *89*, 4255–4271.
(6) Ciabini, L.; Gorelli, F. A.; Santoro, M.; Bini, R.; Schettino, V.; Mezouar, M. *Phys. Rev. B* **2005**, *72*, 094108.
(7) Ciabini, L.; Santoro, M.; Gorelli, F. A.; Bini, R.; Schettino, V.; Raugei, S. *Nature Mater.* **2007**, *6*, 39–43.
(8) Piermarini, G. J.; Mighell, A. D.; Weir, C. E.; Block, S. *Science* **1969**, *165*, 1250–1256.
(9) Katrusiak, A.; Podsiadło, M.; Budzianowski, A. *Cryst. Growth Des.* **2010**, *10*, 3461–3465.
(10) Raiteri, P.; Martonak, R.; Parrinello, M. *Angew. Chem. Int. Ed.* **2005**, *44*, 3769–3773.
(11) Carlsson, A. E.; Ashcroft, N. W. *Phys. Rev. Lett.* **1983**, *50*, 1305.
(12) Ashcroft, N. W. *Phys. Rev. Lett.* **2004**, *92*, 187002.
(13) Zurek, E.; Hoffmann, R.; Ascroft, N. W.; Oganov, A.; Lyakhov, A. *Proc. Natl. Acad. Sci. U.S.A.* **2009**, *106*, 17640–17643.
(14) Yakusheva, B.; Yakushev, V. V.; Dremin, A. N. *High Temp. High Pressure* **1971**, *3*, 261–266.
(15) See the papers cited in ref 7, for example.
(16) Perdew, J. P.; Burke, K.; Ernzerhof, M. *Phys. Rev. Lett.* **1997**, *78*, 1396–1396.
(17) Kresse, G.; Hafner, J. *Phys. Rev. B* **1993**, *47*, 558–561.
(18) Bloechl, P. E. *Phys. Rev. B* **1994**, *50*, 17953–17979.
(19) Kresse, G.; Joubert, D. *Phys. Rev. B* **1999**, *59*, 1758–1775.
(20) Glass, C. W.; Oganov, A. R.; Hansen, N. *Comput. Phys. Commun.* **2006**, *175*, 713–720.
(21) Oganov, A. R.; Glass, C. W. *J. Chem. Phys.* **2006**, *124*, 244704.
(22) Oganov, A. R.; Glass, C. W; Ono, S. *Earth Planet. Sci. Lett.* **2006**, *241*, 95–103.
(23) Lonie, D.; Zurek, E. *Comput. Phys. Commun.* **2011**, *182*, 372–387.
(24) Herzfeld, K. F.; Goeppert Mayer, M. *Phys. Rev. B* **1934**, *46*, 995–1001.
(25) Wodrich, M. D.; Corminboeuf, C.; Schleyer, P. v. R. *Org. Lett.* **2006**, *8*, 3631–3634.
(26) Grimme, S. *J. Comput. Chem.* **2006**, *27*, 1787–1799.
(27) Bučko, T.; Hafner, J.; Lebégue, S.; Ángyán, J. G. *J. Phys. Chem. A* **2010**, *114*, 11814–11824.
(28) Johnson, K. A.; Ashcroft, N. W. *Nature* **2000**, *403*, 632–635.
(29) Huller, M.; Prager, M.; Press, W.; Seydel, T. *J. Chem. Phys.* **2008**, *128*, 034503.
(30) Johnson, R. D.; Yannoni, C. S.; Dorn, H. C.; Salem, J. R.; Bethune, D. S. *Science* **1992**, *255*, 1235–1238.
(31) Nicol, M.; Yin, G. Z. *J. Phys. (Paris)* **1984**, *45* (C8), 163–172.
(32) Drickhamer, H. H. *Science* **1967**, *156*, 1183–1189.
(33) Shaik, S.; Shurki, A.; Danovich, D.; Hiberty, P. *Chem. Rev.* **2001**, *101*, 1501–1539.
(34) From *Handbook of Chemistry and Physics*, all gases at 298 K.
(35) Douglas, J. E.; Rabinovitch, B. S.; Looney, F. S. J. *Chem. Phys.* **1955**, *23*, 315–323.
(36) Blanksby, S. J.; Ellison, G. B. *Acc. Chem. Res.* **2003**, *36*, 255–263.
(37) Sluiter, M. H. F.; Kawazoe, Y. *Phys. Rev. B* **2003**, *68*, 085410.
(38) Sofo, J. O.; Chaudhari, A.; Barber, G. D. *Phys. Rev. B* **2007**, *75*, 153401.
(39) Elias, D. C.; Nair, R. R.; Mohiuddin, T. M. G.; Morozov, S. V.; Blake, P.; Halsall, M. P.; Ferrari, A. C.; Boukhvalov, D. W.; Katsnelson, M. I.; Geim, A. K.; Novoselov, K. S. *Science* **2009**, *323*, 610–613.
(40) Ryu, S.; Han, M. Y.; Maultzsch, J.; Heinz, T. F; Kim, P.; Steigerwald, M. L.; Brus, L. E. *Nano Lett.* **2009**, *8*, 4597–4602.
(41) Wen, X.-D.; Hand, L.; Labet, V.; Yang, T.; Hoffmann, R.; Ashcroft, N. W.; Artem, R. O.; Andriy, O. L. *Proc. Natl. Acad. Sci. U.S.A.* **2011**, *108*, 6833–6837.
(42) Nuspl, G.; Polborn, K.; Evers, J.; Landrum, G. A.; Hoffmann, R. *Inorg. Chem.* **1996**, *35*, 6922–6932 and references therein.
(43) Landrum, G. A.; Hoffmann, R.; Evers, J.; Boysen, H. *Inorg. Chem.* **1998**, *37*, 5754–5763 and references therein.
(44) Bojin, M. D.; Hoffmann, R. *Helv. Chim. Acta* **2003**, *86*, 1653–1682 and references therein.
(45) Rüdorff, W.; Rüddorf, G. *Z. Anorg. Allg. Chem.* **1947**, *253*, 281–296.
(46) Ebert, L. B.; Brauman, J. I.; Huggins, R. A. *J. Am. Chem. Soc.* **1974**, *96*, 7841–7842.
(47) Charlier, J. C.; Gonze, X.; Michenaud, J. P. *Phys. Rev. B* **1993**, *47*, 16162–16168.
(48) Bhattacharya, A.; Bhattacharya, S.; Majumder, C.; Das, G. P. *Phys. Rev. B* **2011**, *83*, 033404.
(49) Leenaerts, O.; Peelaers, H.; Hernández-Nieves, A. D.; Partoens, B.; Peeters, F. M. *Phys. Rev. B* **2010**, *82*, 195436.
(50) Pickard, C. J.; Needs, R. J. *Nature Phys.* **2007**, *3*, 473–476.
(51) Katz, T. J.; Acton, N. *J. Am. Chem. Soc.* **1973**, *95*, 2738–2739.
(52) Katz, T. J.; Wang, E. J. *J. Am. Chem. Soc.* **1971**, *93*, 3782–3783.
(53) Tamelen, E. E. V.; Pappas, S. P. *J. Am. Chem. Soc.* **1962**, *84*, 3789–3791.
(54) Woodward, R. B.; Hoffmann, R. *J. Am. Chem. Soc.* **1965**, *87*, 395–397.

(55) Car, R.; Parrinello, M. *Phys. Rev. Lett.* **1985**, *55*, 2471.
(56) Grochala, W.; Hoffmann, R.; Feng, J.; Ashcroft, N. W. *Angew. Chem. Int. Ed.* **2007**, *46*, 3620–3642.
(57) Wang, Z.; Wen, X.-D.; Hoffmann, R.; Son, J. S.; Li, R.; Fang, C.-C.; Smilgies, D.-M.; Hyeon, T. *Proc. Natl. Acad. Sci. U.S.A.* **2010**, *107*, 17119–17124.
(58) (a) Goldhammer, D. A. *Theorie und ihre Folgerungen*; Teubner: Leipzig, 1913. (b) Herzfeld, K. F. *Phys. Rev.* **1927**, *29*, 701–705.(c) Batsanov, S. S. *Refractometry and Chemical Structure*; Van Nostrand: New York, 1966.
(59) Anderson, P. W. *The Theory of Superconductivity in High-Tc Cuprates*; Princeton University Press: Princeton, NJ, 1997.
(60) Merz, K. M., Jr.; Hoffmann, R.; Balaban, A. T. *J. Am. Chem. Soc.* **1987**, *109*, 6742–6751.
(61) The bulk and shear moduli contain information regarding the hardness of a material with respect to various types of deformation. In this work, the Reuss definition is utilized to compute the bulk and shear moduli: bulk modulus = $(S_{11} + S_{22} + S_{33} + 2(S_{12} + S_{13} + S_{23}))^{-1}$; shear modulus = $15/[4(S_{11} + S_{22} + S_{33} - S_{12} - S_{13} - S_{23}) + 3(S_{44} + S_{55} + S_{66})]$, where S_{ij} (1/GPa) are the elastic compliance constants.
(62) McSkimin, H. J.; Bond, W. L. *Phys. Rev.* **1957**, *105*, 116–121.
(63) Engelke, R. *J. Am. Chem. Soc.* **1986**, *108*, 5799–5803.
(64) Engelke, R.; Hay, P. J.; Klier, D. A.; Wadt, W. R. *J. Am. Chem. Soc.* **1984**, *106*, 5439–5446.
(65) Rogachev, A. Y.; Wen, X.-D.; Hoffmann, R. *Angew Chem. Int. Ed.* **2011**, submitted.
(66) (a) Röttele, H.; Martin, W.; Oth, J. F. M.; Schröder, G. *Chem. Ber.* **1969**, *102*, 3985–3995. (b) Berson, J. A.; Davis, R. F. *J. Am. Chem. Soc.* **1972**, *94*, 3658–3659.
(67) Yang, N. C.; Hrnjez, B. J.; Horner, M. G. *J. Am. Chem. Soc.* **1987**, *109*, 3158–3159.
(68) (a) Braun, R.; Kummer, M.; Martin, H. D.; Rubin, M. B. *Angew. Chem. Int. Ed.* **1985**, *24*, 1059–1060. (b) Bertsch, A.; Grimme, W.; Reinhardt, G. *Angew. Chem. Int. Ed.* **1986**, *25*, 377–378.
(69) Yang, N. C.; Horner, M. G. *Tetrahedron Lett.* **1986**, *27*, 543–546.
(70) Martin, H. D.; Pföhler, P. *Angew. Chem. Int. Ed.* **1978**, *17*, 847–848.
(71) Tim, K.; Srinivasachar, K.; Yang, N. C. *J. Chem. Soc., Chem. Commun.* **1979**, 1038–1040.